



Deposited via The University of Sheffield.

White Rose Research Online URL for this paper:

<https://eprints.whiterose.ac.uk/id/eprint/141691/>

Version: Accepted Version

---

**Article:**

Backman, G., Lawton, B. and Morley, N.A. (2019) Magnetostrictive energy harvesting: materials and design study. IEEE Transactions on Magnetics, 55 (7). 4700206. ISSN: 0018-9464

<https://doi.org/10.1109/TMAG.2019.2891118>

---

© 2019 IEEE. Personal use of this material is permitted. Permission from IEEE must be obtained for all other users, including reprinting/ republishing this material for advertising or promotional purposes, creating new collective works for resale or redistribution to servers or lists, or reuse of any copyrighted components of this work in other works. Reproduced in accordance with the publisher's self-archiving policy.

**Reuse**

Items deposited in White Rose Research Online are protected by copyright, with all rights reserved unless indicated otherwise. They may be downloaded and/or printed for private study, or other acts as permitted by national copyright laws. The publisher or other rights holders may allow further reproduction and re-use of the full text version. This is indicated by the licence information on the White Rose Research Online record for the item.

**Takedown**

If you consider content in White Rose Research Online to be in breach of UK law, please notify us by emailing [eprints@whiterose.ac.uk](mailto:eprints@whiterose.ac.uk) including the URL of the record and the reason for the withdrawal request.

# Magnetostrictive Energy Harvesting: Materials and design study

Gary Backman, Ben Lawton, and Nicola A Morley, *Member, IEEE*

Department of Materials Science and Engineering, University of Sheffield, Sheffield, UK, S1 3JD

In recent years, vibrational energy harvesting has established itself as a promising alternative to the use of batteries for powering microelectromechanical systems (MEMS) for large wireless sensor networks used in aerospace and building infrastructures. This work has focused on the design and materials used in magnetostrictive cantilever energy harvesters. The study involved using both finite element modelling to predict the resonance frequencies for different cantilever designs and magnetostrictive materials, followed by experimental measurements for validation. Two different magnetostrictive ribbons were investigated,  $\text{Fe}_{100-x}\text{Ga}_x$  with four different compositions ( $x = 17.5; 19.5; 21; 28 \text{ at.}\%$ ) and amorphous metallic glass Metglas 2605SC ( $\text{Fe}_{81}\text{B}_{13.5}\text{Si}_{3.5}\text{C}_2$ ). From the modelling, it was determined that the resonance frequency was strongly dependent on the cantilever length, thickness and density. Changing the cantilever design to a “T” shape was found to decrease the resonance frequency. The experimental results found that the output voltage measured depended on the cantilever dimensions especially the thickness, the Ga concentration and the cantilever design. The output voltages for  $\text{Fe}_{80.5}\text{Ga}_{19.5}$  cantilevers were comparable with the same dimension Metglas cantilevers. The results of the finite element modelling were validated by good agreement between the computational and experimental resonance frequencies measured.

*Index Terms*— magnetostriction, Metglas, Fe-Ga, energy harvesting.

## I. INTRODUCTION

IN INDUSTRIES such as aerospace, healthcare, and building infrastructures, wireless sensor networks (WSNs) are being used to monitor environmental and physical conditions [1, 2]. They use arrays of microelectromechanical systems (MEMS) sensors, each monitoring a small area, from which data can be collected and combined to provide a comprehensive overview of the system. WSNs are favoured as they reduce the amount of wiring required and hence the cost, energy and weight of a monitoring system. To establish these WSNs, each MEMS device must be powered separately. Traditionally this is done by batteries, although this is not cost-effective in the long run due to the finite life of the battery. Replacing the batteries can be near impossible for inaccessible sensors or time-consuming for large arrays of 1000’s of sensors. One option is to use energy harvesting devices in each sensor, thus making them self-sufficient. At present, energy harvesters provide only the fraction of the power which batteries do; but with recent technological advances in integrated circuit fabrication, reduced power CMOS circuitry, and very large scale integration design, the power consumption of conventional wireless sensors has been reduced, thus making energy harvesters a viable option [3].

There are a number of different types of energy harvesters, including thermal and vibrational [4, 5]. The most common vibrational ones are piezoelectric energy harvesters [6] but

draw backs include piezoelectric layer depoling during use, having a brittle material nature and having poor coupling. Magnetostrictive energy harvesters are less common as they require a pick-up coil but don’t suffer from depolarisation and can have a high coupling constant (Table 1). The basic design of a magnetostrictive energy harvester consists of a cantilever made of a magnetostrictive material, which oscillates within a pick-up coil [3, 7]. The induced voltage in the pick-up coil can then be used to power the MEMS devices. Often additional electronic circuits are required to amplify the output voltage from the coils. Much of the work on magnetostrictive energy harvesters has focussed on using Metglas ribbon as the cantilever [3, 7] and determining how the cantilever dimensions including thickness influence the maximum output voltage and power.

Hu *et al* [7] studied the effect of different numbers of Metglas layers on the output voltage, mechanical damping and natural resonant frequencies. They found that as the number of layers increased, the mechanical damping increased. The first natural frequency linearly changed from 68Hz for 1 layer to ~80Hz for 8 layers, while the third natural frequency linearly increased from ~800Hz for 1 layer to ~1400 Hz for 8 layers, showing that the dependence on the number of Metglas layers increases for higher order natural frequencies. For the output voltage, the maximum value depended on both the number of layers as well as the order of natural frequency. For example, at the first natural frequency, 4 layers gave the largest output voltage, while for the 3rd order natural frequency, 1 layer gave the largest output voltage, with the voltage then decreasing as the number of layers increased. Thus showing that there are a wide range of variables upon which the output voltage depends. Chiriac *et al* [8] studied a range of nanocrystalline ribbons in the classic magnetostrictive energy harvester design. Different processing techniques such as annealing were used to produce amorphous and nanocrystalline ribbons, which were then used in an energy harvester set-up to determine which gave the best output. It was found that the nanocrystalline ribbons gave the best results.

Manuscript received April 1, 2015; revised May 15, 2015 and June 1, 2015; accepted July 1, 2015. Date of publication July 10, 2015; date of current version July 31, 2015. (Dates will be inserted by IEEE; “published” is the date the accepted preprint is posted on IEEE Xplore®; “current version” is the date the typeset version is posted on Xplore®). Corresponding author: N. A. Morley (e-mail: n.a.morley@sheffield.ac.uk). G. Backwell and B. Lawton contributed equally.

Color versions of one or more of the figures in this paper are available online at <http://ieeexplore.ieee.org>.

Digital Object Identifier (inserted by IEEE).

Ueno *et al* [9] were the first to investigate Fe-Ga ribbons in energy harvesters. They used the composition  $\text{Fe}_{81.6}\text{Ga}_{18.4}$  in a parallel beam arrangement. For 1mm x 0.5mm x 10mm cantilevers, the first natural resonance was at 395Hz with a maximum power output of 2mW. This is significantly higher than that found for Metglas 2605SC by Wang *et al* [3] who, in their experimental configuration, achieved a maximum power output of 576 $\mu$ W at a higher frequency of 1.1kHz. Ueno *et al* also showed that for free vibration characteristics, the energy conversion increased with resonant frequency, such that at 94Hz the efficiency was 5.4%, while at 395Hz the efficiency was 16%.

Another magnetostrictive material investigated in energy harvesters is Terfenol-D, which is an alloy with the composition  $\text{Tb}_{0.3}\text{Dy}_{0.7}\text{Fe}_{1.9}$ . It has the advantage of having a large magnetostriction constant ( $\lambda_s \sim 1200\text{ppm}$ ) but has a lower tensile strength (28MPa [10]), which is a factor 20 smaller than other alloys such as Fe-Ga (515MPa [11]), thus often has had to be used in composite designs. Terfenol-D has been studied in a range of magnetostrictive energy harvesters, including transducers [12] and PZT composite cantilevers [13, 14].

Magnetostrictive energy harvesters can also consist of a rod of magnetostrictive material, which are either used to harvest the energy from falling mass [15] or use a transducer set-up [12, 16]. Davino *et al* [15] demonstrated an energy harvester, which consisted of a Terfenol-D rod with a pick-up coil, within a solenoid applying a bias field along the rod. The rod was strained by a 200g free falling mass, giving the rod a mechanical excitation, which was measured on the pick-up coil.

Berbyuk [16] and Staley *et al* [12] studied low frequency transducer energy harvesters. Staley *et al* studied an energy harvesting transducer which consisted of a magnetostrictive cylindrical rod (either Galfenol or Terfenol-D) within a pick up and along with a biasing coil. The design used a supported free beam to apply a dynamic stress to the rod. The output voltage was measured on the pick-up coils as a function of the frequency of the applied stress and the magnitude of the bias field. The aim was to successfully demonstrate an energy harvester that could work at 50Hz. They found that the Galfenol performed better within the transducer than the Terfenol-D for the same mechanical inputs. Berbyuk *et al* also studied Galfenol and Terfenol-D in a magnetostrictive transducer. The magnetostrictive rod in this system was subjected to compressive force at both ends, with a permanent biasing magnet at one end. The output was measured on a set-up of pick-up coils. They studied how the output voltage changed as a function of frequency, pre-stress and biasing field. It was found that the output voltage could be maximised by optimising the pre-stress and biasing field. Also, Galfenol was found to have a higher practical potential compared to Terfenol-D.

Another design of a magnetostrictive energy harvester, was presented by Zucca *et al* [17]. They used pre-stressed  $\text{Fe}_{78}\text{B}_{13}\text{Si}_9$  strips. Five strips were stacked together, then were subjected to axial vibrations. A pick-up coil around the ribbon

converted the change in magnetisation into an electrical signal. A biasing permanent magnet was placed under the ribbon to improve the performance. They achieved a power of  $\sim 3\mu\text{W}/\text{cm}^3$  at 300Hz. A more comprehensive review of the different types of magnetostrictive energy harvesters is found in the review paper by Deng *et al* [18].

## INSERT TABLE 1 HERE

The aim of this research was to study the design and materials used in magnetostrictive energy harvesters, including directly comparing Fe-Ga alloys with Metglas to determine whether any of the Fe-Ga compositions were a good alternative and whether a “T” bar design had advantages over the classic cantilever design. Metglas was chosen as it has previously been used in magnetostrictive energy harvesters [3, 7] and is commercially available, while Fe-Ga is a relatively new magnetostrictive material, which has a higher magnetostriction constant (table 1), therefore a comparison between the two allows for a greater understanding of the role of the magnetostrictive material in the energy harvester. When designing an energy harvester, there are two important issues to consider, the first is the frequency of the vibration being harnessed, and the second is the size of the energy harvester. In general, the vibration frequency is often below 100Hz, while the resonance frequency of a cantilever increases with decreasing size. Therefore to minimise the size of the energy harvester, while maintaining a low resonance frequency requires the design of the cantilever to be studied. Therefore in this paper, a “T” bar design along with the classic cantilever design was investigated. The “T” bar was chosen, as it is a simple design, so is easy to fabricate and allowed weight to be added to the end of the cantilever to achieve lower frequencies. Also the pick-up coil was designed to fit around the cantilever’s long part, with the bar part outside the coil. This meant that the size of the coil and “T” bar cantilever was the same as the classic cantilever.

## II. EXPERIMENTAL SET-UP

### A. Multiphysics Modelling

The finite element modelling software COMSOL Multiphysics was used to predict the resonance frequency of the different cantilever designs, along with how the material properties such as density change the behaviour. Fig. 1 shows the basic set-up of the model for both the classic cantilever and the “T” bar design, with the cantilever fixed at one end. The functional parameters were taken from table 1. The density of the Fe-Ga ribbon used in the modelling was determined from the actual Fe-Ga ribbons used in the experimental part. The modelling included two different thickness, (18 $\mu\text{m}$  and 60 $\mu\text{m}$ ) of Metglas ribbon and 50  $\mu\text{m}$  thick Fe-Ga ribbon, along with the “T” bar design using 60 $\mu\text{m}$  thick Metglas. The first study investigated the material parameters, with the cantilever dimensions in the length range of 45mm to 55 mm and width range of 4mm to 6mm. The second study investigated a wider length (10mm to 100mm)

and width (5mm to 20mm) range. For each cantilever, the first six resonance frequencies (Eigenfrequencies) were determined (Fig. 1). These consisted of both bending and twisting resonance frequencies, depending on the dimensions of the cantilever. Preliminary simulations were carried out to determine the optimum mesh size for the cantilever, as too coarse a mesh gave large variation within the resonance frequencies, but too fine a mesh resulted in excessive computing times.

### INSERT FIG 1 HERE

#### B. Experimental Procedure

For the magnetostrictive energy harvesters, two different Fe-based alloys were studied in ribbon form. The Fe-Ga ribbons were produced by the melt-spinning method at the National Institute of R&D for Technical Physics, Iasi, Romania. The four ribbon composition studied were  $\text{Fe}_{100-x}\text{Ga}_x$  ( $x = 17.5; 19.5; 21; 28$  at.%) with thicknesses of 45-50  $\mu\text{m}$  and widths of  $5 \pm 1$  mm. The Metglas 2605SC ribbon was brought from Metglas Inc and had a thickness of 18  $\mu\text{m}$ . As the thickness of the ribbon influences the resonant frequency of the cantilever [18], three Metglas ribbons were bonded together using a cyanoacrylate adhesive to produce a cantilever of thickness 54  $\mu\text{m}$  for comparison with the similar Fe-Ga thick cantilevers. The adhesive was chosen to try and ensure that the natural resonance frequencies of the 3 layer cantilever were comparable to the single layer thickness and were not dominated by the material properties of the adhesive. For the material study, the overall dimensions of the cantilevers were  $50 \pm 1 \text{mm} \times 5 \pm 1 \text{mm}$ . A summary of the ribbons studied is given in table 1, along with their main properties. From table 1, it is observed that although the Young's modulus and magnetomechanical coupling factor of Fe-Ga ribbons are smaller than Metglas, the magnetostriction constant is a factor of 10 higher, and the Curie Temperature is double those of Metglas. These properties could be favourable for aerospace applications, where the working temperatures may exceed 300K. To check the structure of the Fe-Ga ribbons, x-ray diffraction (XRD) was carried out. A Siemens D5000 instrument was used with a Cu source, with  $K_{\alpha 1}$  and  $K_{\alpha 2}$  radiations averaging to a wavelength  $\lambda = 1.5418 \text{ \AA}$ , and  $1^\circ$  divergence and anti-scatter slits. Data were collected over the angular range  $20-120^\circ 2\theta$  at 3 sec/step. The specimens were rotated during data collection. It was determined that all the Fe-Ga ribbons were crystalline, with lattice constants linearly increasing from 2.896  $\text{ \AA}$  for 17.5% Ga to 2.901  $\text{ \AA}$  for 21% Ga, then staying constant at 2.901  $\text{ \AA}$  for 28% Ga. The Metglas ribbon was amorphous.

For the different cantilever design study, Metglas sheet of thickness 60  $\mu\text{m}$  was used. This was for two reasons, the first was from the results of the materials study it was found that the 18  $\mu\text{m}$  thick ribbon was too flexible to be used as a cantilever. The second, it allowed the "T" bar shaped cantilevers to be cut as a single cantilever, rather than having to glue the bar part onto the cantilever length. For the classic cantilever design, the width was varied between 2.5mm to

10mm and the length was varied between 10 to 50mm, while for the "T" bar design, the "T" width was varied between 5 to 25mm (Fig. 1).

### INSERT FIG 2 HERE

The basic principle of the comparison measurement was to vibrate the different magnetostrictive cantilevers over a frequency range within a pick-up coil (Fig. 2). The cantilevers were vibrated using a loudspeaker (Visaton WS 17E or Visaton FR12), which was powered using a 4V peak to peak sine wave from the output of a Stanford Research systems lock-in amplifier. The input vibration signal to the loudspeaker was measured over the frequency range to ensure that it was the same for all the ribbons. No variation in the input signal was measured. The voltage across the speaker was measured (Fig 2 inset), observing a peak at around 40Hz due to the resonance of the speaker. The pick-up coil was connected to the same lock-in amplifier, to measure the output voltage across it. The lock-in amplifier was set to measure the signal magnitude. For these measurements no additional electronic circuit, such as the voltage multiplication circuit used by Hu *et al* [7], was used between the pick-up coil and the lock-in. This means that the output voltages presented in this paper have not been amplified nor optimised. The pick-up coil had dimensions of  $30 \times 70 \times 16 \text{ mm}^3$ , with 850 turns.

The background voltage of the experiment (i.e. the voltage across the pick-up coil with no ribbon in the coil) was measured, to determine the resonant frequency of the loudspeaker and the background drift on the measured voltage. This was carried out before and after every measurement. Fig. 2b shows the measured background voltage, and it is observed for the speaker that there is a small peak at 40Hz, the first resonance frequency of the loudspeaker, with two further peaks at 77Hz and 188Hz. The same increase in voltage was observed as the frequency was increased for all measurements, thus showing the increase in voltage to be independent of the experimental set-up. It is likely that this observation is a result of drift on the lock-in amplifier used, as this was the only unchanged part of the experiment. The loudspeaker background was subtracted from the output voltages measured for the cantilevers.

### III. RESULTS AND DISCUSSION

Fig. 3 shows the COMSOL modelling results for the different materials and designs studied. The resonance frequency can be changed by changing both the dimensions of the cantilever, the design and the material properties. For the Fe-Ga cantilevers, changing the width of the cantilever by 1mm, did not affect the resonance frequency, but as observed in Fig 3a, changing the length by 1mm or thickness by 2  $\mu\text{m}$  changed the resonance frequency. For the Fe-Ga (50mm x 5mm) cantilever, the resonance frequency changes by 5Hz for a length difference of 2mm and by 4Hz for a thickness difference of 2  $\mu\text{m}$ . While the density of the ribbon also changed the resonance frequency (Fig. 3b), a difference in  $1500 \text{ kgm}^{-3}$ , which is the difference in density between

19.5%Ga and 29%Ga ribbons gave a change in resonance frequency of 10Hz. This means that to use the modelling to design magnetostrictive cantilevers, it is important to know all the material parameters. For the Metglas cantilevers (Figs 3c and d), the bending and twisting modes of the cantilever both occur at frequencies less than 200Hz. The cantilever twisting modes resonance frequencies are dependent on the width of the cantilever, while the bending modes resonance frequencies are independent of the width. For a Metglas 50mm x 5mm cantilever, the second or higher resonance frequencies strongly depend upon the thickness, as for 18 $\mu$ m the 2nd bending resonance is 34.6Hz compared to 92Hz for 60 $\mu$ m. While the 1st resonance frequency is almost independent of thickness, as the two frequencies were 16.5Hz (18 $\mu$ m) and 15.3Hz (60 $\mu$ m). This means when designing a magnetostrictive cantilever, the thickness (and therefore the stiffness) should be taken account of, if the working resonance frequency is the second or above. It is also observed that there is a large increase in the resonance frequency as the cantilever length is decreased below 30mm, which means that trying to miniaturise these devices is more difficult. Thus the “T” bar design was modelled to determine whether this would help solve the problem. For an overall length of 20mm, it is observed that the 1st resonance frequency dropped from 15Hz for no “T” bar to 10 Hz for a “T” bar of dimensions 5mm x 20mm and the 2nd resonance frequency from 92Hz to 79Hz. Thus the shape of the “T” has helped to reduce the resonance frequency. It is also observed that the bending resonance frequencies slowly decrease as the “T” bar part increases in size, while the twisting frequencies decrease more rapidly.

### INSERT FIG 3 HERE

Fig. 4 shows the experimental resonance frequencies for the different cantilevers investigated in the study. For the Fe-Ga cantilevers it is observed that the 2nd resonance frequency measured is in the range 69Hz (19% Ga) to 74Hz (28% Ga), while the 1st resonance frequency is just observable at 12Hz for the 19%Ga, but was not measured for any other Fe-Ga composition. The magnitude of the resonance changes as a function of Ga composition, with the 19% Ga having the largest voltage output. This coincides with the ribbon having the largest magnetostriction constant ( $\lambda \sim 395$ ppm), while the 21% and 28% Ga composition ribbons have the lowest output voltage and they also have smaller magnetostriction constants (table 1). This suggests that the magnitude of the output voltage depends upon the magnetostriction constant, which in Fe-Ga ribbons depends upon the Ga concentration.

### INSERT FIG 4 HERE

For the 18 $\mu$ m and 3x18 $\mu$ m Metglas cantilevers (Fig. 4b), it is observed that the resonance frequency of the speaker produced a larger peak in the data, than the 2nd natural resonance frequencies of the cantilevers themselves. For the Fe-Ga cantilevers, the speaker resonance frequency peak was much smaller than the peak observed in the Metglas

cantilevers' frequency sweep. One possible reason for this is that the 18 $\mu$ m Metglas cantilever thickness was much thinner than the Fe-Ga cantilevers, and therefore more flexible so responded to the speaker resonance greater than the Fe-Ga cantilevers. It should also be noted for the 60 $\mu$ m Metglas cantilevers, no speaker resonance was measured.

Comparison can also be made between the different thicknesses of Metglas cantilevers studied. The 3x18 $\mu$ m Metglas cantilever total thickness is almost the same as the 60 $\mu$ m thick Metglas cantilever. Thus comparing the results of the 50mm x 5mm cantilevers, it is observed for the 60 $\mu$ m cantilever, three bending resonances were measured at 5Hz, 25Hz and 75Hz, while for the 3x18 $\mu$ m Metglas cantilever, two resonances were measured at  $\sim$  10Hz and 78Hz. Thus both of these cantilevers have a resonance at around 75Hz. The magnitude of the output voltage also depended on the thickness of the Metglas cantilevers. For 50mm x 5mm cantilevers, at the 2<sup>nd</sup> resonance frequency, the output voltage for the 18 $\mu$ m cantilever was 0.86mV compared to 0.36mV for the 3x18 $\mu$ m cantilever and 0.06mV for the 60  $\mu$ m cantilever. Thus it decreased as the thickness of the cantilever increased. The 20mm x 5mm x 60 $\mu$ m Metglas cantilever output voltage was 0.23mV, so comparable with the 3x18 $\mu$ m Metglas cantilever. For the Fe-Ga cantilevers, the 19% Ga ribbon had the largest output voltage of 0.97mV, thus is comparable to the 18 $\mu$ m Metglas cantilever and better than the 3x18 $\mu$ m Metglas cantilever, therefore making Fe-Ga ribbons an alternative to Metglas for magnetostrictive cantilevers.

For the classic Metglas 60 $\mu$ m cantilever, the resonance frequency depended strongly on the length (Fig. 4c), but not on the width. It was found that changing the width from 2.5mm to 10mm, only changed the resonance frequency from 26Hz to 29Hz. Therefore confirming the modelling data, that the cantilever width does not change the 1st bending frequency of the cantilevers. While changing the length from 10mm to 50mm changed the frequency from 170Hz to 5Hz, again confirming the modelling prediction that the resonance frequency strongly changes for lengths below 20mm. It was also found that the output voltage depended on the length of the cantilever, with the longer cantilevers having smaller output voltages compared to the shorter ones. This was observed to be due to the longer cantilevers “drooping” within the pick-up coils, meaning at resonance they were unable to resonant at the same magnitude as the shorter cantilevers, hence a lower output voltage was measured. This means to achieve larger output voltages the cantilever should be stiff. Also the 10mm cantilever had a lower output voltage, due to having less material compared to the 20mm cantilever.

For the “T” bar cantilever, the width of the “T” influenced the resonance frequency and the output voltage (Fig. 4d). It was found that the additional mass on the end of the cantilever due to the “T” shape meant the cantilever was bent when stationary rather than horizontally straight, i.e a similar situation to the longer classic cantilevers. This again lowered the output voltage measured for the larger “T” designs. Comparing the resonance frequencies between the classic cantilever and the “T” bar, it is observed the resonance

frequency does decrease with increasing width of the “T”. The 5mm “T” width is the classic cantilever with no “T” part, thus the resonance frequency can be shifted by 10 Hz with the addition of the “T”, but the output voltage decreases by a factor 3. Therefore although the “T” bar in theory should help with the minimization of the cantilever, in practice, it does not provide as high an output voltage as the classic cantilever.

#### INSERT FIG 5 HERE

Finally the experimental results are compared with the modelling predictions. For the Fe-Ga cantilevers (Fig. 5a), it is observed that there is good agreement with the resonance frequency of the 50mm length cantilevers with the modelling predictions, while for the shorter cantilevers the measured resonance frequencies were lower than the predicted ones. Similarly for the 60 $\mu$ m Metglas cantilevers as a function of length, the measured resonance frequencies are all lower than the predicted frequencies. Although the trends observed in the resonance frequencies, i.e. much higher frequencies for shorter cantilevers were observed. Also the modelling predicted that the width of the cantilever would not change the resonance frequency, and experimentally no difference in the resonance frequency was measured for the different width cantilevers. This means that the modelling was able to predict a trend in the resonance frequencies and a “ball-park” value for them, but if one of the materials parameters such as density (Fig. 3b) or the dimensions (Fig. 3a) are wrong in the model, then the predicted frequency will be different from the experiments.

For the T-bar cantilevers, the measured resonance frequencies were higher than the predicted frequencies, but the decrease in resonance frequency with increase in T-bar width was measured. Thus the modelling was able to predict that the “T” bar was a possible design to achieve a smaller cantilever, with a lower resonance frequency. The reason for the difference between the modelling and the experimental results again could be due to incorrect material parameters in the model or error in the fabrication of the cantilever. The cantilevers were cut out of large sheets of Metglas, thus any error in the length or width of the cantilever or “T” bar design will change the resonance frequency, as discussed above.

#### IV. CONCLUSIONS

It has been shown that trends in resonance frequency of magnetostrictive cantilevers can be predicted using COMSOL modelling, with frequency values strongly dependent on the cantilever dimensions and material parameters. Experimentally, the output voltage measured strongly depends upon the dimensions and design of the cantilever along with the magnetostrictive material used. It was shown that Fe-Ga (19% Ga) ribbon had competitive outputs compared to Metglas cantilevers of the same dimensions. While the output voltage decreased for Fe-Ga ribbons with lower magnetostriction constants. To reduce the resonance frequency, without increasing the size of the cantilever, the “T” bar design was investigated. It was found that for a total

cantilever length of 20mm, the resonance frequency could be reduced by 10Hz with the additional of a 5mm x 20mm “T” on the end. The disadvantage was that the output voltage decreased as well with the addition of the “T” part.

#### ACKNOWLEDGEMENTS

NAM wishes to thank N. Lupu and her group at the National Institute of R&D for Technical Physics, Iasi, Romania, for the fabrication of the Fe-Ga ribbons.

#### REFERENCES

- [1] G. J. Pottie, “Wireless Sensor Networks”, in International Telecoms Week, Killarney, Ireland, 1998
- [2] National Instruments Corporation, “What is a wireless sensor network?”, 5/5/2012 (Online)
- [3] L. Wang and F. G. Yuan, “Vibration Energy harvesting by Magnetostrictive Materials”, *Smart Materials & Structures*, vol 17, no 4, 2008
- [4] N. G. Stephen, “On Energy Harvesting from Ambient Vibrations”, *Journal of Sound and vibration*, vol. 293, no. 1-2, pp. 409-425, 2006
- [5] H. A. Sodano, G. E. Simmers, R. Dereux and D. J. Inman, “Recharging batteries using Energy Harvested from Thermal gradients”, *Journal of Intelligent Material Systems and Structures*, vol. 18, no. 1, pp. 3-10, 2007
- [6] C. R. Bowen, H. A. Kim, P. M. Weaver and S. Dunn, “Piezoelectric and ferroelectric materials and structures for energy harvesting applications”, *Energy and Environmental Science*, vol. 7, no. 1, pp. 25-44, 2014
- [7] J. Hu, F. Xu, A. Q. Huang and F. G. Yuan, “Optimal Design of vibration-based energy harvester using magnetostrictive material (MsM)”, *Smart Materials and Structures*, vol. 20, no. 1, 2011
- [8] H. Chiriac, M. Tibu, N. Lupu, I. Skorvanek and T.-A. Ovari, “Nanocrystalline ribbons for energy harvesting applications”, *Journal of Applied Physics*, vol. 115, pp. 17A320, 2014
- [9] T. Ueno and S. Yamada, “Performance of Energy Harvester Using Iron-Gallium Alloy in Free Vibration”, *IEEE Transactions of Magnetics*, vol. 47, no. 10, pp. 2407-2409, 2011
- [10] A. E. Nolting and E. Summers, “Tensile properties of binary and alloyed Galfenol”, *Journal of Materials Science*, vol. 50, pp. 5136-5144, 2015
- [11] Etrema USA Terfenol Data sheet
- [12] M E Staley and A B Flatau, “Characterisation of energy harvesting potential of Terfenol-D and Galfenol” *Smart Structures and Materials*, vol. 5764, pp. 630 - 640, 2005
- [13] T. Lafont, L. Gimeno, J. Delamare, G. A. Lebedev, D. I. Zakharov, B. Viala, O. Cugat, N. Galopin, L. Garbuio and O. Geoffroy, “Magnetostrictive-piezoelectric composite structures for energy harvesting”, *J. Micromech. Microeng.* Vol. 22, pp. 094009, 2012
- [14] X. Dai, Y. Wen, P. Li, J. Yang and G. Zhang, “Modeling characterization and fabrication of vibration energy harvester using Terfenol-D/PZT/Terfenol-D composite transducer”, *Sensors and Actuators A: Physical*, vol. 156, pp. 350-358, 2009
- [15] D. Davino, A. Giustiniani, C. Visone and A. Adly, “Experimental analysis of vibrations damping due to magnetostrictive based energy harvesting” *Journal of Applied Physics*, vol. 109, pp. 07E509, 2011
- [16] V. Berbyuk, “Vibration energy harvesting using Galfenol based transducer”, *Active and Passive Smart Structures and Integrated Systems*, vol. 8688, pp. 1F-1, 2013
- [17] M. Zucca, O. Bottauscio, C. Beatrice, A. Hadadian, F. Fiorillo and L. Martino, “A study on Energy Harvesting by amorphous strips”, *IEEE transactions on magnetics*, vol. 50, no. 11, pp. 8002104, 2014
- [18] Z. Deng and M. J. Dapino, “Review of magnetostrictive vibration energy harvesters”, *Smart Materials and Structures*, vol. 26, pp. 103001, 2017
- [19] M. Ali, “Growth and Study of Magnetostrictive FeSiBC thin films for device applications”, PhD thesis, University of Sheffield, Sheffield, 1999
- [20] S. Datta, J. Atulasimha, C. Mudivartha and A. B. Flatau, “Stress and magnetic field-dependent Young’s modulus in single crystal iron-gallium alloys”, *Journal of magnetism and magnetic materials*, vol 322, pp. 2135 – 2144, 2010

[21] A. E. Clark, K. B. Hathaway, M. Wun-Fogle, J. B. Restorff, V. M. Keppens, G. Petculescu and R. A. Taylor, "Extraordinary magnetoelasticity and lattice softening in bcc Fe-Ga alloys", *Journal of Applied Physics*, vol. 93, pp. 10, 2003

[22] A. E. Clarke, M. Wun-Fogle, J. B. Restorff, T. A. Lograsso and J. R. Cullen, "Effect of quenching on the magnetostriction of  $Fe_{1-x}Ga_x$  ( $0.13 < x < 0.21$ )", *IEEE transactions on Magnetics*, vol. 37, no 4, pp. 2678-2680, 2001

[23] J. Atulasimha and A. B. Flatau, "A review of magnetostrictive iron-gallium alloys", *Smart Materials and Structures*, vol. 20 pp. 4, 2011

[24] G. D. Liu, X. F. Dai, Z. H. Liu, J. L. Chen and G. H. Wu, "Structure, magnetostriction and magnetic properties of melt-spun Fe-Ga alloys", *Journal of Applied Physics*, vol. 99, pp. 093904, 2006

[25] A. E. Clark, M. Wun-Fogle, J. B. Restorff, K. W. Dennis, T. A. Lograsso and R. W. McCallum, "Temperature dependence of the magnetic anisotropy and magnetostriction of  $Fe_{100-x}Ga_x$  ( $x=8.6, 16.6, 28.5$ )", *Journal of Applied Physics*, vol. 97, pp. 10M316, 2005

[26] L.B. Chen, X. X. Zhu, C. A. Li, J. H. Liu, C. B. Jiang and H. B. Xu, "<001> oriented single crystal growth and magnetostriction of  $Fe_{81}Ga_{19}$  alloys", *Acta Metallurgica Sinica*, vol. 47, no. 2, pp. 169-172, 2011

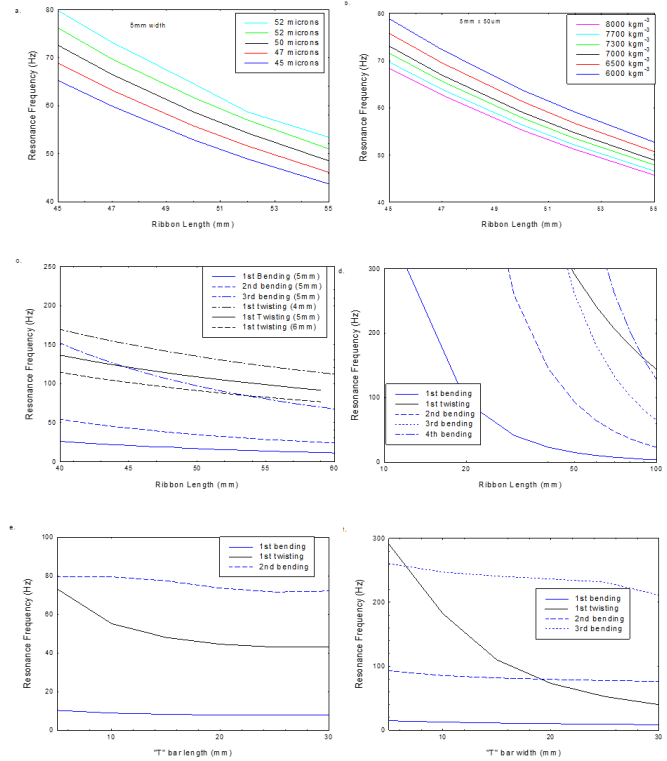


Fig. 3. COMSOL results for magnetostrictive cantilevers with width 5mm for FeGa cantilevers with a. different thicknesses and b. different density, for Metglas cantilevers with c. different widths and thickness 18 $\mu$ m and d. different lengths with thickness 60 $\mu$ m, and for "T" bar cantilevers with e. different length "T" and f. different width "T" and thickness 60 $\mu$ m

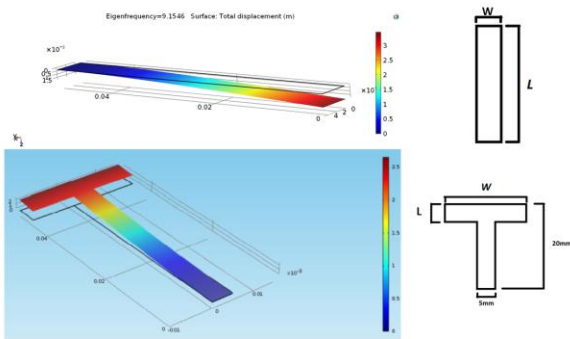


Fig. 1. COMSOL modelling a. simple cantilever design and b. the "T" bar design

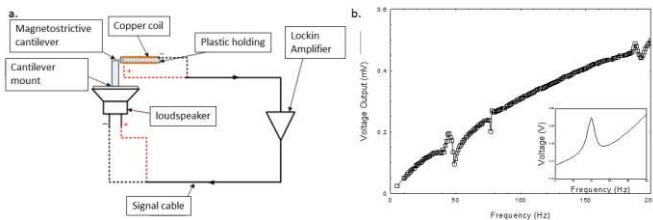


Fig. 2. Experimental set-up and background output voltage. Inset: voltage across the speaker as a function of frequency

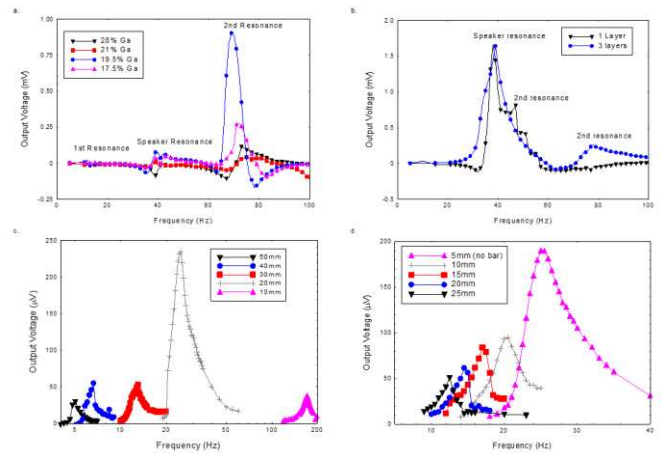


Fig. 4. Voltage as a function of frequency for a. FeGa cantilevers, b. Metglas cantilevers (layer thickness 18 $\mu$ m), c. Metglas cantilevers (layer thickness 60 $\mu$ m) and d. Metglas T-bar cantilevers

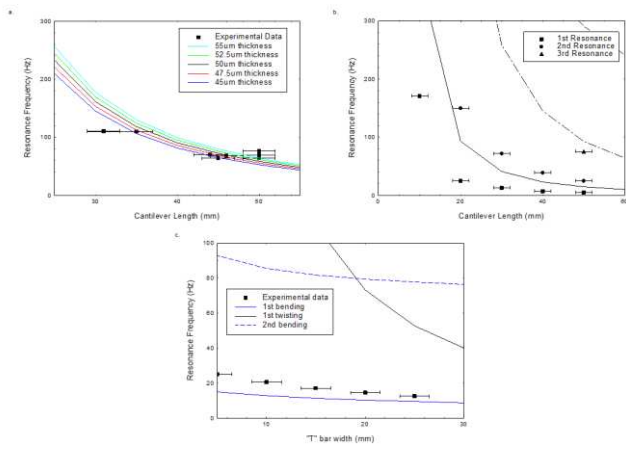


Fig. 5. Comparison between the modelling data and the resonance frequency for different dimension cantilevers a. FeGa, b. Metglas (layer thickness 60µm) and c. “T” bar cantilevers

TABLE I  
MATERIAL PROPERTIES OF METGLAS AND FE-GA RIBBONS

Material Property	Metglas 2605SC	Fe <sub>82.5</sub> Ga <sub>17.5</sub>	Fe <sub>80.5</sub> Ga <sub>19.5</sub>	Fe <sub>79</sub> Ga <sub>21</sub>	Fe <sub>72</sub> Ga <sub>28</sub>
Young's Modulus (GPa)	160±40 [19]	65 [20]	59 [20]	-	30 [20]
Magnetostriction constant (ppm)	~30 [19]	320 [21]	395 [21]	274 [21]	305 [21]
Saturation Magnetisation (kA/m)	128 [19]	143 [22]	135 [22]	119 [22]	90 [25]
Magneto-mechanical coupling factor	0.97 [19]	~0.66 [23]	~0.66 [23]	~0.66 [23]	~0.66 [23]
Curie Temperature (°C)	370-380 [19]	720 [24]	690 [24]	640 [24]	400 [24]
Anisotropy (kJm <sup>-3</sup> )	38 [19]	27 [25]	13 [26]	-	~1 [25]